International Journal of Solids and Structures 50 (2013) 3586–3596

Contents lists available at SciVerse ScienceDirect

International Journal of Solids and Structures

journal homepage: www.elsevier.com/locate/ijsolstr

Finite-amplitude shear horizontal waves propagating in a pre-stressed layer between two half-spaces

Priza Kayestha [a], Elizabete Rodrigues Ferreira [b,c], Anil C. Wijeyewickrema [a,*]

[a] Department of Civil and Environmental Engineering, Tokyo Institute of Technology, 2-12-1, O-okayama, Meguro-ku, Tokyo 152-8552, Japan
[b] Département de Mathématique, Université Libre de Bruxelles, Campus Plaine CP218/1, 1050 Bruxelles, Belgium
[c] Department of Mechanical, Aerospace and Nuclear Engineering, Rensselaer Polytechnic Institute, Troy, NY 12180, USA

ARTICLE INFO

Article history:
Received 10 September 2012
Received in revised form 24 June 2013
Available online 15 July 2013

Keywords:
Compressible
Dispersion curves
Finite-amplitude waves
Non-linear elasticity
Pre-stress

ABSTRACT

The propagation of finite-amplitude time-harmonic shear horizontal waves, in a pre-stressed compressible elastic layer of finite thickness embedded between two identical compressible elastic half-spaces, is investigated. This is accomplished by combining finite-amplitude linearly polarized inhomogeneous transverse plane wave solutions in the half-spaces and finite-amplitude linearly polarized unattenuated transverse plane wave solutions in the layer. The layer and half-spaces are made of different pre-stressed compressible neo-Hookean materials. The dispersion relation which relates wave speed and wavenumber is obtained in explicit form. The special case where the interfaces between the layer and the half-spaces are principal planes of the left Cauchy–Green deformation tensor is also investigated. Numerical results are presented showing the variation of the shear horizontal wave speed with the pre-stress and the propagation angle.

1. Introduction

The propagation of finite-amplitude waves in pre-stressed elastic solids, which give rise to a constitutive non-linearity, has gained attention since the early 1960s and there are useful analytical results available in the literature. However, the exact results available are much sparser, when compared to the studies on infinitesimal wave propagation in pre-stressed elastic solids. A good overview of infinitesimal waves and finite-amplitude waves propagating in pre-stressed elastic materials is given by Destrade and Saccomandi (2005, 2010). Finite-amplitude homogeneous as well as inhomogeneous waves have been investigated previously, for both incompressible and compressible pre-stressed elastic solids. Here, the review of previous work will be limited to the propagation of finite-amplitude waves in pre-stressed *compressible* elastic solids which is of interest in the present paper.

For pre-stressed compressible elastic media, the propagation of finite-amplitude homogeneous plane waves was studied prior to the propagation of finite-amplitude inhomogeneous plane waves. John (1966) and Currie and Hayes (1969) showed that three linearly polarized finite-amplitude homogeneous waves, one longitudinal and two transverse, can propagate in any direction in a pre-stressed Hadamard material. Boulanger et al. (1994) also studied finite-amplitude homogeneous wave propagation in a pre-stressed Hadamard material and showed that finite-amplitude circularly polarized transverse homogeneous waves can propagate in this material along special directions called *acoustic axes*. The acoustic axes are determined by the static deformation of the material and are independent of the choice of the material constants and the material function which occur in the strain energy function describing the Hadamard material.

One of the first researchers to consider the propagation of finite-amplitude time-harmonic *inhomogeneous* plane waves in pre-stressed compressible elastic media was Destrade (1999). He investigated the propagation of finite-amplitude linearly polarized time-harmonic inhomogeneous transverse plane waves in a pre-stressed special Blatz-Ko material, sometimes also called compressible neo-Hookean material or restricted Hadamard material. These waves are polarized in the direction **a** perpendicular to both the propagation direction **n** and the attenuation direction **m**. He showed that such waves can propagate in the material only if **n** and **m** are conjugate with respect to the strain ellipsoid associated with **B**, i.e., when $\mathbf{n}\cdot\mathbf{B}\mathbf{m}=0$, where **B** is the left Cauchy–Green deformation tensor corresponding to the static homogeneous deformation. Later, Rodrigues Ferreira and Boulanger (2005) also investigated the propagation of finite-amplitude linearly polarized inhomogeneous transverse plane waves in a pre-stressed special Blatz-Ko material, but without assuming that they are time-harmonic. They showed that for all given unit vectors **n** and **m** (**m** not along **n**), linearly polarized transverse *damped* inhomogeneous plane waves may propagate. Such waves are attenuated

* Corresponding author. Tel.: +81 3 5734 2595; fax: +81 3 5734 3478.
E-mail address: wijeyewickrema.a.aa@m.titech.ac.jp (A.C. Wijeyewickrema).

0020-7683/$ - see front matter © 2013 Elsevier Ltd. All rights reserved.
http://dx.doi.org/10.1016/j.ijsolstr.2013.07.002

(or amplified) both in space and time, and the term damped refers to an exponential decay (or growth) with time. In the special case when $\mathbf{n}\cdot\mathbf{Bm}=0$, they retrieved the solution obtained by Destrade (1999). The possibility of the superposition of finite-amplitude transverse inhomogeneous plane waves and longitudinal waves in a pre-stressed special Blatz-Ko material was investigated by Rodrigues Ferreira and Boulanger (2007). They showed that the superposition of a finite-amplitude transverse inhomogeneous wave and a longitudinal wave is also a solution, in the case when the propagation direction of the longitudinal wave is perpendicular to the polarization direction of the transverse wave. All these studies considered finite-amplitude wave propagation in a pre-stressed unbounded elastic medium. In Rodrigues Ferreira et al. (2008), a problem with boundaries was presented, where they considered the propagation of finite-amplitude Love waves in a pre-stressed elastic layer of finite thickness overlying a half-space both made of different compressible neo-Hookean materials. A finite-amplitude Love wave solution is obtained provided the propagation direction in the interface and the normal to the interface are conjugate with respect to the strain ellipsoid associated with the left Cauchy–Green deformation tensor.

In the present paper, the propagation of finite-amplitude shear horizontal waves in a pre-stressed compressible elastic layer embedded between two identical compressible elastic half-spaces is investigated, by combining finite-amplitude linearly polarized inhomogeneous transverse wave solutions in the half-spaces and finite-amplitude linearly polarized unattenuated transverse wave solutions in the layer. This kind of configuration can be encountered for instance in adhesively bonded structures characterized by a layer embedded between two half-spaces. Therefore, exact analytical results can be useful when adhesively bonded structures are examined using non-destructive methods based on propagation of elastic waves. Moreover, the configuration considered in the manuscript, i.e., a layer embedded between two half-spaces, can be considered as a limiting case of a symmetric layered composite consisting of an inner layer of thickness d and two identical outer layers of thickness h, in the limit when $h\gg d$. This same configuration was investigated by Stoneley (1924) and Ewing et al. (1954) for the corresponding case of time harmonic infinitesimal wave propagation in a stratum of uniform thickness bounded on both sides by very deep layers of different materials.

The layer and the half-spaces are made of different compressible neo-Hookean materials. The full Hadamard material involves two constitutive constants C and D (John, 1966). The compressible neo-Hookean material considered here, which is also called restricted Hadamard, is a special case with $D=0$ and $C=\mu$ (Willson, 1977). It is noted that the results obtained here are possible because the compressible neo-Hookean material does not give rise to normal stresses. Normal stresses would yield additional boundary conditions, which cannot be satisfied in context of this paper. The constitutive equation for compressible neo-Hookean material and the equations of motion are presented in Section 2. In Section 3, the displacement fields for finite-amplitude linearly polarized inhomogeneous transverse wave motion and finite-amplitude linearly polarized unattenuated transverse plane wave motion are obtained. In Section 4, the geometry of the problem is described in which a pre-stressed compressible elastic layer is embedded between pre-stressed compressible elastic half-spaces rigidly bonded at the interfaces. It is shown that the left Cauchy–Green deformation tensors in the half-spaces can be obtained uniquely when the left Cauchy–Green deformation tensor in the layer is known. The dispersion relation is obtained in explicit form provided that the direction of the normal to the plane of constant phase $\mathbf{n}$ and the direction of the normal to the plane of constant amplitude $\mathbf{m}$ are conjugate with respect to the strain ellipsoid associated with the left Cauchy–Green deformation tensor. Dispersion curves are presented for a particular choice of material parameters which show an explicit dependence on the underlying deformation. In Section 5, the special case when the interfaces are principal planes of the left Cauchy–Green deformation tensor is considered, where the propagation of finite-amplitude shear horizontal waves is possible along any direction in the principal plane. Numerical results are presented showing the variation of the shear horizontal wave speed with the pre-stress and the propagation angle.

2. Governing equations for compressible neo-Hookean material

The governing equations for finite-amplitude time-harmonic waves propagating in a pre-stressed compressible neo-Hookean material are given in this section. A homogeneous, compressible isotropic elastic body is considered which when unstressed occupies the configuration $\mathcal{B}_u$ This body is subjected to a large static homogeneous deformation

$$\mathbf{x}=\mathbf{F}\mathbf{X},\quad x_i=F_{iR}X_R,\quad (i,R=1,2,3), \tag{1}$$

which results in a pre-stressed equilibrium configuration $\mathcal{B}_e$ where $\mathbf{F}$ is the deformation gradient tensor, $\mathbf{X}$ is the position vector of a particle in the undeformed configuration and $\mathbf{x}$ is the corresponding position vector in the intermediate state of static deformation. The associated left Cauchy–Green deformation tensor $\mathbf{B}$ is given by

$$\mathbf{B}=\mathbf{F}\mathbf{F}^{\mathrm{T}}. \tag{2}$$

The strain energy function $W_c^{(\mathrm{nH})}$, of a compressible neo-Hookean material, also called 'special Blatz-Ko material' or 'restricted Hadamard material', measured per unit volume in the undeformed state is given by

$$2W_c^{(\mathrm{nH})}=\mu(\mathrm{tr}\,\mathbf{B}-3)+G(J)-G(1), \tag{3}$$

where μ is the shear modulus and $G(J)$ is a function of J in which $J=\det\mathbf{F}$. From Eq. (3), the symmetric Cauchy stress tensor $\mathbf{T}$ is given by (Beatty, 1996),

$$\mathbf{T}=\frac{1}{2}G'(J)\mathbf{I}+\mu J^{-1}\mathbf{B}, \tag{4}$$

where $\mathbf{I}$ is the identity tensor. It has been shown by Hayes (1968) that the constitutive equation for Hadamard material reduces to the constitutive equation given in Eq. (4), when the ordered forces inequalities and the strong ellipticity conditions are satisfied. Here, for compressible neo-Hookean material, the strong ellipticity conditions

$$\mu>0,\quad G''(J)\geqslant 0, \tag{5}$$

are assumed to hold. Since the configuration $\mathcal{B}_u$ is assumed to be stress free with $J=1$ and $\mathbf{B}=\mathbf{I}$, $G'(1)=-2\mu$. In addition, comparison with linearized elasticity yields $G''(1)=2(\lambda+\mu)$, where λ and μ are the Lamé parameters (Boulanger et al., 1994).

To the large static homogeneous deformation given in Eq. (1), a finite-amplitude time-dependent displacement $\mathbf{u}(\mathbf{x},t)$ is superimposed and the body thus occupies a time-dependent deformed configuration $\mathcal{B}_t$ The particle at $\mathbf{x}$ in the intermediate state of static deformation then moves to $\bar{\mathbf{x}}$ which is given by

$$\bar{\mathbf{x}}=\mathbf{x}+\mathbf{u}(\mathbf{x},t). \tag{6}$$

The deformation gradient tensor $\bar{\mathbf{F}}$ with respect to the undeformed configuration is given by

$$\bar{\mathbf{F}}=\partial\bar{\mathbf{x}}/\partial\mathbf{X}=\hat{\mathbf{F}}\mathbf{F}, \tag{7}$$

where $\hat{\mathbf{F}}=\partial\bar{\mathbf{x}}/\partial\mathbf{x}$ is the deformation gradient tensor with respect to the intermediate state of static deformation. The corresponding left Cauchy–Green deformation tensor $\bar{\mathbf{B}}$ is given by

$$\bar{\mathbf{B}} = \bar{\mathbf{F}}\bar{\mathbf{F}}^{\mathrm{T}} = \hat{\mathbf{F}}\mathbf{B}\hat{\mathbf{F}}^{\mathrm{T}}. \tag{8}$$

The equations of motion in the absence of body forces can be written as

$$\mathrm{div}_{\bar{\mathbf{x}}}\bar{\mathbf{T}} = \bar{\rho}\ddot{\bar{\mathbf{x}}}, \quad \frac{\partial \bar{T}_{ij}}{\partial \bar{x}_j} = \bar{\rho}\ddot{\bar{x}}_i \quad (i,j=1,2,3), \tag{9}$$

where $\mathrm{div}_{\bar{\mathbf{x}}}$ corresponds to the divergence operator with respect to the position $\bar{\mathbf{x}}$, $\bar{\mathbf{T}}$ is the Cauchy stress tensor at time t, $\bar{\rho} = \rho_0/\bar{J}$ is the mass density at time t in which ρ_0 is the mass density in the undeformed state and $\bar{J} = \det\bar{\mathbf{F}}$. Note that a superimposed dot indicates differentiation with respect to time t. The first Piola–Kirchhoff stress tensor $\bar{\mathbf{P}}$ at time t with respect to the intermediate state of static deformation is given by

$$\bar{\mathbf{P}} = \hat{J}\bar{\mathbf{T}}\hat{\mathbf{F}}^{-\mathrm{T}}, \tag{10}$$

where $\hat{J} = \det\hat{\mathbf{F}}$. The equations of motion given in Eq. (9) can thus be written as

$$\mathrm{div}_{\mathbf{x}}\bar{\mathbf{P}} = \rho\ddot{\bar{\mathbf{x}}}, \quad \frac{\partial \bar{P}_{ij}}{\partial x_j} = \rho\ddot{\bar{x}}_i \quad (i,j=1,2,3), \tag{11}$$

where $\mathrm{div}_{\mathbf{x}}$ corresponds to the divergence operator with respect to the position $\mathbf{x}$, and $\rho = \rho_0/J$ is the mass density in the intermediate state of static deformation.

3. Transverse wave motion in a homogeneously deformed body

In this section, transverse wave solutions in pre-stressed compressible elastic neo-Hookean material are considered (see Rodrigues Ferreira et al., 2008). The finite-amplitude linearly polarized transverse inhomogeneous plane waves are propagating with wave speed v in the direction of $\mathbf{n}$, polarization is in the transverse direction $\mathbf{a}$ with the amplitude varying along the direction of $\mathbf{m}$. The superimposed finite-amplitude time-dependent displacement field $\mathbf{u}(\mathbf{x},t) = \bar{\mathbf{x}} - \mathbf{x}$ is thus given by

$$\mathbf{u}(\mathbf{x},t) = f(\mathbf{m}\cdot\mathbf{x})g(\mathbf{n}\cdot\mathbf{x} - vt)\mathbf{a}, \tag{12}$$

where $\mathbf{n}$, $\mathbf{a}$, $\mathbf{m}$ are unit vectors and f and g are real functions to be determined. It is assumed that the unit vectors $\mathbf{m}$ and $\mathbf{n}$ are not parallel and that the polarization direction $\mathbf{a}$ is orthogonal to both $\mathbf{m}$ and $\mathbf{n}$ such that

$$\mathbf{a}\cdot\mathbf{m} = \mathbf{a}\cdot\mathbf{n} = 0. \tag{13}$$

In Eq. (12), the planes defined by $\mathbf{m}\cdot\mathbf{x} =$ constant are the planes of constant amplitude and the planes defined by $\mathbf{n}\cdot\mathbf{x} =$ constant are the planes of constant phase.

For the wave motion given by Eq. (12), the deformation gradient tensor $\hat{\mathbf{F}}$ with respect to the intermediate state of static deformation yields

$$\begin{aligned}\hat{\mathbf{F}} &= \mathbf{I} + f'g(\mathbf{a}\otimes\mathbf{m}) + fg'(\mathbf{a}\otimes\mathbf{n}),\\ \hat{\mathbf{F}}^{-1} &= \mathbf{I} - f'g(\mathbf{a}\otimes\mathbf{m}) - fg'(\mathbf{a}\otimes\mathbf{n}),\end{aligned} \tag{14}$$

and

$$\det\hat{\mathbf{F}} = 1, \tag{15}$$

where f' and g' denote the derivatives of f and g with respect to their argument. The Cauchy stress tensor at time t for the pre-stressed compressible neo-Hookean material can then be written as

$$\bar{\mathbf{T}} = \frac{1}{2}G'(J)\mathbf{I} + \mu J^{-1}\hat{\mathbf{F}}\mathbf{B}\hat{\mathbf{F}}^{\mathrm{T}}. \tag{16}$$

Hence, the first Piola–Kirchhoff stress tensor $\bar{\mathbf{P}}$ at time t given in Eq. (10) yields

$$\bar{\mathbf{P}} = \frac{1}{2}G'(J)\hat{\mathbf{F}}^{-\mathrm{T}} + \mu J^{-1}\hat{\mathbf{F}}\mathbf{B}. \tag{17}$$

Then, substituting Eqs. (6), (12), and (17) into the equations of motion Eq. (11) yields

$$\rho v^2 fg''\mathbf{a} = \mu J^{-1}(f''g\,\mathbf{m}\cdot\mathbf{B}\mathbf{m} + 2f'g'\,\mathbf{n}\cdot\mathbf{B}\mathbf{m} + fg''\,\mathbf{n}\cdot\mathbf{B}\mathbf{n})\mathbf{a}. \tag{18}$$

Substituting $\rho = \rho_0/J$, it can be shown that the displacement given in Eq. (12) is the solution of the equations of motion, if and only if the functions f and g satisfy the equation

$$(\mathbf{n}\cdot\mathbf{B}\mathbf{n} - \mu^{-1}\rho_0 v^2)fg'' + 2\mathbf{n}\cdot\mathbf{B}\mathbf{m}f'g' + \mathbf{m}\cdot\mathbf{B}\mathbf{m}f''g = 0. \tag{19}$$

The unit vectors $\mathbf{m}$ and $\mathbf{n}$ are chosen such that

$$\mathbf{n}\cdot\mathbf{B}\mathbf{m} = 0, \tag{20}$$

which implies that the unit vectors $\mathbf{m}$ and $\mathbf{n}$ are conjugate with respect to the $\mathbf{B}$-ellipsoid $\mathbf{x}\cdot\mathbf{B}\mathbf{x} = 1$. Eq. (19), thus yields two uncoupled equations for the functions f and g,

$$v_{\mathbf{m}}^2(f''/f) = -b, \quad (v_{\mathbf{n}}^2 - v^2)(g''/g) = b, \tag{21}$$

where b is an arbitrary constant, $v_{\mathbf{m}}$ and $v_{\mathbf{n}}$ are the wave speeds of homogeneous bulk waves propagating along $\mathbf{m}$ and $\mathbf{n}$, respectively, and given by

$$\rho_0 v_{\mathbf{m}}^2 = \mu\,\mathbf{m}\cdot\mathbf{B}\mathbf{m}, \quad \rho_0 v_{\mathbf{n}}^2 = \mu\,\mathbf{n}\cdot\mathbf{B}\mathbf{n}. \tag{22}$$

With the assumption that b is negative, let $b = -\gamma^2$ for some real γ, then Eq. (21) yields a linearly polarized *inhomogeneous* time-harmonic transverse plane wave if $v^2 < v_{\mathbf{n}}^2$. The displacement field of this wave is

$$\mathbf{u}(\mathbf{x},t) = A\exp\left(-\frac{\gamma}{v_{\mathbf{m}}}\mathbf{m}\cdot\mathbf{x}\right)\cos\left(\frac{\gamma}{\sqrt{v_{\mathbf{n}}^2 - v^2}}(\mathbf{n}\cdot\mathbf{x} - vt)\right)\mathbf{a}, \tag{23}$$

where γ and A are arbitrary constants. If b is assumed to be positive, let $b = \kappa^2$ for some real κ, then Eq. (21) yields a linearly polarized *unattenuated* time-harmonic transverse plane wave if $v^2 > v_{\mathbf{n}}^2$. The displacement field of this wave is

$$\mathbf{u}(\mathbf{x},t) = \left[B\sin\left(\frac{\kappa}{v_{\mathbf{m}}}\mathbf{m}\cdot\mathbf{x}\right) + C\cos\left(\frac{\kappa}{v_{\mathbf{m}}}\mathbf{m}\cdot\mathbf{x}\right)\right]\cos\left(\frac{\kappa}{\sqrt{v^2 - v_{\mathbf{n}}^2}}(\mathbf{n}\cdot\mathbf{x} - vt)\right)\mathbf{a}, \tag{24}$$

where κ, B and C are arbitrary constants. Note that when the condition given in Eq. (20) is not satisfied, other solutions may be obtained (see Rodrigues Ferreira and Boulanger, 2005) but they are not time-harmonic. In this paper, the interest is in time-harmonic shear horizontal waves.

Note that the traction vector $\mathbf{t}$ on the plane $\mathbf{m}\cdot\mathbf{x} =$ constant can be shown to be the same whether it is measured per unit area of the intermediate state of static deformation or per unit area of the current state (Rodrigues Ferreira et al., 2008) and is given by

$$\mathbf{t} = \bar{\mathbf{P}}\mathbf{m} = \bar{\mathbf{T}}\mathbf{m} = \mathbf{T}\mathbf{m} + \rho v_{\mathbf{m}}^2 f' g\,\mathbf{a}. \tag{25}$$

4. SH waves propagating in a pre-stressed layer between two half-spaces

A compressible isotropic elastic layer of finite thickness is considered to be embedded between two identical compressible isotropic elastic half-spaces. The layer and the half-spaces are homogeneous and made of different compressible neo-Hookean material with material parameters and mass density $\tilde{\mu}$, $\tilde{G}$, $\tilde{\rho}_0$ and μ, G, ρ_0, respectively. In the remainder of the paper, all quantities with a tilde refer to variables and parameters of the layer. The layer

is assumed to be rigidly bonded to the half-spaces. The origin O lies at the interface of the layer and the lower half-space.

4.1. Pre-stressed equilibrium state

The elastic layer and the half-spaces are subjected to a large static homogeneous deformation such that the half-spaces are identical even after the deformation. The initial deformations are given by,

$$\tilde{\mathbf{x}} = \tilde{\mathbf{F}}\mathbf{X} \quad \text{and} \quad \mathbf{x} = \mathbf{F}\mathbf{X}, \tag{26}$$

where $\mathbf{X}$ denotes the position vector of material particle in the undeformed solids. The associated left Cauchy–Green deformation tensors for the pre-stressed layer and the half-spaces are given by

$$\tilde{\mathbf{B}} = \tilde{\mathbf{F}}\tilde{\mathbf{F}}^{\mathrm{T}} \quad \text{and} \quad \mathbf{B} = \mathbf{F}\mathbf{F}^{\mathrm{T}}. \tag{27}$$

The unit vector $\mathbf{m}$ is taken to be normal to the faces of the layer, in the intermediate state of static deformation. As shown in Fig. 1, the lower half-space occupies the space $\mathbf{m}\cdot\mathbf{x} \geqslant 0$, the layer occupies the region $-h \leqslant \mathbf{m}\cdot\tilde{\mathbf{x}} \leqslant 0$ and the upper half-space occupies the space $\mathbf{m}\cdot\mathbf{x} \leqslant -h$. The focus here is on the finite-amplitude time-harmonic shear horizontal waves, propagating in a direction $\mathbf{n}$ and polarized in a transverse direction $\mathbf{a}$, both parallel to the interface. Thus, the unit vectors $\mathbf{n}$, $\mathbf{a}$ and $\mathbf{m}$ form an orthonormal triad. Since the layer and the half-spaces are rigidly bonded, displacements and tractions are continuous at the interfaces. Using these continuity conditions, the left Cauchy–Green deformation tensor $\mathbf{B}$ in the half-spaces can be determined uniquely when the left Cauchy–Green deformation tensor $\tilde{\mathbf{B}}$ in the layer is known (Rodrigues Ferreira et al., 2008) and will be briefly discussed here. In previous studies of *infinitesimal* wave propagation in pre-stressed elastic layered media, each medium was subjected to different pre-stress conditions (Wijeyewickrema and Leungvichcharoen, 2009; Kayestha et al., 2010). In these studies, the continuity of stress component perpendicular to the interface had been used to obtain the stretches in that direction, however, the stretches in the other directions were prescribed independently in each medium.

In the pre-stressed equilibrium state, at the interfaces $\mathbf{m}\cdot\mathbf{x} = \mathbf{m}\cdot\tilde{\mathbf{x}} = 0$ and $\mathbf{m}\cdot\mathbf{x} = \mathbf{m}\cdot\tilde{\mathbf{x}} = -h$, the continuity of the displacement and the traction vector can be written as

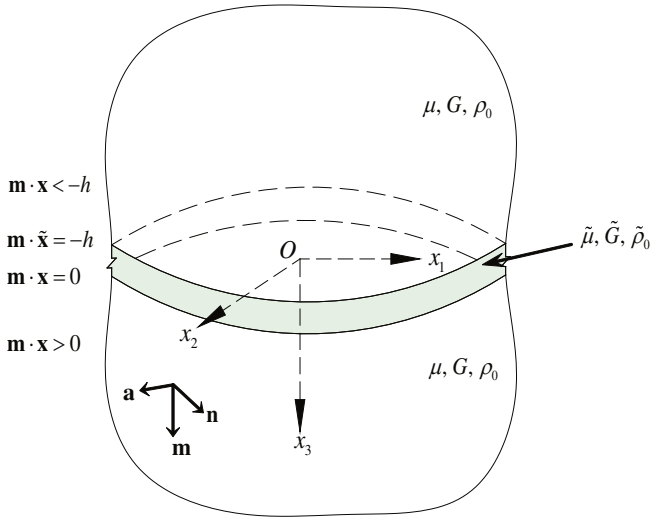

Fig. 1. Pre-stressed layer between two identical half-spaces. Wave propagation is in the direction of $\mathbf{n}$, polarization is in the transverse direction $\mathbf{a}$ and the amplitude varies along the direction $\mathbf{m}$, normal to the faces of the layer. Here, $\mathbf{n}$, $\mathbf{a}$, $\mathbf{m}$ are unit vectors.

$$\mathbf{u}(\mathbf{x}) = \tilde{\mathbf{u}}(\tilde{\mathbf{x}}) \quad \text{and} \quad \mathbf{T}\mathbf{m} = \tilde{\mathbf{T}}\mathbf{m}. \tag{28}$$

The displacement in the half-spaces is given by

$$\mathbf{u}(\mathbf{x}) = \mathbf{x} - \mathbf{X} = (\mathbf{I} - \mathbf{F}^{-1})\mathbf{x}, \tag{29}$$

and the displacement in the layer can be written as

$$\tilde{\mathbf{u}}(\tilde{\mathbf{x}}) = \tilde{\mathbf{x}} - \mathbf{X} = (\mathbf{I} - \tilde{\mathbf{F}}^{-1})\tilde{\mathbf{x}}. \tag{30}$$

At the interface $\mathbf{m}\cdot\mathbf{x} = \mathbf{m}\cdot\tilde{\mathbf{x}} = 0$, the position vector can be written as, $\mathbf{x} = \tilde{\mathbf{x}} = p\mathbf{n} + q\mathbf{a}$, while at the interface $\mathbf{m}\cdot\mathbf{x} = \mathbf{m}\cdot\tilde{\mathbf{x}} = -h$, it can be written as $\mathbf{x} = \tilde{\mathbf{x}} = p\mathbf{n} + q\mathbf{a} - h\mathbf{m}$, for arbitrary p and q. Then, the continuity of the displacement given in Eq. (28a) at $\mathbf{m}\cdot\mathbf{x} = \mathbf{m}\cdot\tilde{\mathbf{x}} = 0$ yields

$$\mathbf{F}^{-1}(p\mathbf{n} + q\mathbf{a}) = \tilde{\mathbf{F}}^{-1}(p\mathbf{n} + q\mathbf{a}). \tag{31}$$

Since Eq. (31) should hold for all p and q, the displacement continuity results in

$$\mathbf{F}^{-1}\mathbf{n} = \tilde{\mathbf{F}}^{-1}\mathbf{n}, \quad \mathbf{F}^{-1}\mathbf{a} = \tilde{\mathbf{F}}^{-1}\mathbf{a}. \tag{32}$$

From Eq. (32),

$$\mathbf{F}^{-1}\mathbf{n} \times \mathbf{F}^{-1}\mathbf{a} = \tilde{\mathbf{F}}^{-1}\mathbf{n} \times \tilde{\mathbf{F}}^{-1}\mathbf{a}. \tag{33}$$

Then, using the identity $\mathbf{F}^{-1}\mathbf{n} \times \mathbf{F}^{-1}\mathbf{a} = (\det\mathbf{F})^{-1}\mathbf{F}^{\mathrm{T}}(\mathbf{n} \times \mathbf{a})$, (Chadwick, 1999) and similarly for $\tilde{\mathbf{F}}$, yields

$$(\det\mathbf{F})^{-1}\mathbf{F}^{\mathrm{T}}\mathbf{m} = (\det\tilde{\mathbf{F}})^{-1}\tilde{\mathbf{F}}^{\mathrm{T}}\mathbf{m}, \tag{34}$$

which gives

$$J^{-2}\mathbf{m}\cdot\mathbf{B}\mathbf{m} = \tilde{J}^{-2}\mathbf{m}\cdot\tilde{\mathbf{B}}\mathbf{m}. \tag{35}$$

Similarly, at the interface $\mathbf{m}\cdot\mathbf{x} = \mathbf{m}\cdot\tilde{\mathbf{x}} = -h$, the displacement continuity yields the same expression as shown in Eq. (35). Making use of the Nanson's formula, the unit vector $\mathbf{M}$ normal to the faces of the layer in the undeformed state is given by

$$\mathbf{M} = (\mathbf{m}\cdot\mathbf{B}\mathbf{m})^{-1/2}\mathbf{F}^{\mathrm{T}}\mathbf{m} = (\mathbf{m}\cdot\tilde{\mathbf{B}}\mathbf{m})^{-1/2}\tilde{\mathbf{F}}^{\mathrm{T}}\mathbf{m}, \tag{36}$$

and the thickness of the layer in the undeformed state is

$$H = h(\mathbf{m}\cdot\tilde{\mathbf{B}}\mathbf{m})^{-1/2}. \tag{37}$$

Next, using the continuity of the traction given in Eq. (28b) at the interfaces $\mathbf{m}\cdot\mathbf{x} = \mathbf{m}\cdot\tilde{\mathbf{x}} = 0$ and $\mathbf{m}\cdot\mathbf{x} = \mathbf{m}\cdot\tilde{\mathbf{x}} = -h$ yields

$$\mu J^{-1}\mathbf{n}\cdot\mathbf{B}\mathbf{m} = \tilde{\mu}\tilde{J}^{-1}\mathbf{n}\cdot\tilde{\mathbf{B}}\mathbf{m}, \tag{38}$$

$$\mu J^{-1}\mathbf{a}\cdot\mathbf{B}\mathbf{m} = \tilde{\mu}\tilde{J}^{-1}\mathbf{a}\cdot\tilde{\mathbf{B}}\mathbf{m}, \tag{39}$$

and

$$\frac{1}{2}G'(J) + \mu J^{-1}\mathbf{m}\cdot\mathbf{B}\mathbf{m} = \frac{1}{2}\tilde{G}'(\tilde{J}) + \tilde{\mu}\tilde{J}^{-1}\mathbf{m}\cdot\tilde{\mathbf{B}}\mathbf{m}. \tag{40}$$

Eq. (40) can be used to obtain J for the half-space using Eq. (35) and because $\tilde{\mathbf{B}}$ is given, J and $\mathbf{m}\cdot\mathbf{B}\mathbf{m}$ are known. In Rodrigues Ferreira et al. (2008), the uniqueness for the determination of J in the half-space has been discussed. It was shown, using the strong ellipticity conditions, that Eq. (40) has at most one positive solution for J, and it has one and only one solution if in addition the assumption $\lim_{J\to 0} G'(J) = -\infty$ is made. After J is obtained, the components of $\mathbf{B}$ can be determined from Eqs. (35), (38), and (39). The remaining components of $\mathbf{B}$ i.e. $\mathbf{a}\cdot\mathbf{B}\mathbf{a}$, $\mathbf{n}\cdot\mathbf{B}\mathbf{n}$ and $\mathbf{n}\cdot\mathbf{B}\mathbf{a}$ can be determined using Eq. (32) resulting from the displacement continuity. In order to use the exact wave solutions described in the previous section, the condition given in Eq. (20) is assumed to be satisfied in the layer, which by Eq. (38) implies that it is also satisfied in the half-spaces. Thus,

$$\mathbf{n}\cdot\tilde{\mathbf{B}}\mathbf{m} = 0, \quad \mathbf{n}\cdot\mathbf{B}\mathbf{m} = 0. \tag{41}$$

Using Eq. (41), the components of the left Cauchy–Green deformation tensor $\mathbf{B}$ are now given by

$$\mathbf{m}\cdot\mathbf{B}\mathbf{m} = (J/\tilde{J})^2\,\mathbf{m}\cdot\tilde{\mathbf{B}}\mathbf{m}, \tag{42}$$

$$\mathbf{a}\cdot\mathbf{B}\mathbf{m} = (\tilde{\mu}/\mu)(J/\tilde{J})\,\mathbf{a}\cdot\tilde{\mathbf{B}}\mathbf{m}, \tag{43}$$

$$\mathbf{a}\cdot\mathbf{B}\mathbf{a} = \mathbf{a}\cdot\tilde{\mathbf{B}}\mathbf{a} + \frac{(\mathbf{a}\cdot\tilde{\mathbf{B}}\mathbf{m})^2}{\mathbf{m}\cdot\tilde{\mathbf{B}}\mathbf{m}}\left(\frac{\tilde{\mu}^2}{\mu^2}-1\right), \tag{44}$$

$$\mathbf{n}\cdot\mathbf{B}\mathbf{n} = \mathbf{n}\cdot\tilde{\mathbf{B}}\mathbf{n}, \tag{45}$$

$$\mathbf{n}\cdot\mathbf{B}\mathbf{a} = \mathbf{n}\cdot\tilde{\mathbf{B}}\mathbf{a}. \tag{46}$$

Using Eqs. (42)–(46), the left Cauchy–Green deformation tensor $\mathbf{B}$ can be written in tensorial form in terms of $\tilde{\mathbf{B}}$ from which it can be shown that $\mathbf{B}\mathbf{n} = \tilde{\mathbf{B}}\mathbf{n}$ (Rodrigues Ferreira et al., 2008).

4.2. Finite-amplitude shear horizontal wave

In this section, finite-amplitude shear horizontal waves propagating with the wave speed v are investigated by combining the solutions of the finite-amplitude linearly polarized inhomogeneous transverse plane wave motion and the finite-amplitude linearly polarized unattenuated transverse plane wave motion given in Eqs. (23) and (24), respectively. In the pre-stressed upper and lower half-spaces, since the waves decay in the direction of the unit vector $\mathbf{m}$, the displacement field given in Eq. (23) is considered. The displacement field in the lower half-space $\mathbf{u}^{\mathrm{LH}}(\mathbf{x},t)$ is thus given by

$$\mathbf{u}^{\mathrm{LH}}(\mathbf{x},t) = A\exp(-s_1\mathbf{m}\cdot\mathbf{x})\cos(k(\mathbf{n}\cdot\mathbf{x}-vt))\mathbf{a}, \tag{47}$$

where A is an arbitrary constant, and the displacement field in the upper half-space $\mathbf{u}^{\mathrm{UH}}(\mathbf{x},t)$ is thus given by

$$\mathbf{u}^{\mathrm{UH}}(\mathbf{x},t) = D\exp(s_1\mathbf{m}\cdot\mathbf{x})\cos(k(\mathbf{n}\cdot\mathbf{x}-vt))\mathbf{a}, \tag{48}$$

where D is an arbitrary constant. In the pre-stressed layer, the displacement field given in Eq. (24) is considered. The displacement field in the layer $\tilde{\mathbf{u}}(\mathbf{x},t)$ is thus given by

$$\tilde{\mathbf{u}}(\mathbf{x},t) = (B\sin(s_2\mathbf{m}\cdot\mathbf{x}) + C\cos(s_2\mathbf{m}\cdot\mathbf{x}))\cos(k(\mathbf{n}\cdot\mathbf{x}-vt))\mathbf{a}. \tag{49}$$

In Eqs. (47)–(49), the following notations have been introduced

$$s_1 = k\sqrt{\frac{v_{\mathbf{n}}^2-v^2}{v_{\mathbf{m}}^2}} = \frac{\gamma}{v_{\mathbf{m}}}, \quad s_2 = k\sqrt{\frac{v^2-\tilde{v}_{\mathbf{n}}^2}{\tilde{v}_{\mathbf{m}}^2}} = \frac{\kappa}{\tilde{v}_{\mathbf{m}}}, \tag{50}$$

where

$$k = \frac{\gamma}{\sqrt{v_{\mathbf{n}}^2-v^2}} = \frac{\kappa}{\sqrt{v^2-\tilde{v}_{\mathbf{n}}^2}}, \tag{51}$$

is the wavenumber. The wavenumber in the displacement fields of the half-spaces and the layer has to be same in order to satisfy the continuous interface conditions. Recalling Eq. (22), the homogeneous bulk wave speeds $v_{\mathbf{m}}$, $v_{\mathbf{n}}$, $\tilde{v}_{\mathbf{m}}$ and $\tilde{v}_{\mathbf{n}}$ propagating along $\mathbf{m}$ and $\mathbf{n}$ in the half-spaces and in the layer, respectively, are given by

$$\begin{aligned} &\rho_0 v_{\mathbf{m}}^2 = \mu\,\mathbf{m}\cdot\mathbf{B}\mathbf{m}, \quad \rho_0 v_{\mathbf{n}}^2 = \mu\,\mathbf{n}\cdot\mathbf{B}\mathbf{n},\\ &\tilde{\rho}_0\tilde{v}_{\mathbf{m}}^2 = \tilde{\mu}\,\mathbf{m}\cdot\tilde{\mathbf{B}}\mathbf{m}, \quad \tilde{\rho}_0\tilde{v}_{\mathbf{n}}^2 = \tilde{\mu}\,\mathbf{n}\cdot\tilde{\mathbf{B}}\mathbf{n}, \end{aligned} \tag{52}$$

and the shear horizontal wave speed v has to satisfy

$$\tilde{v}_{\mathbf{n}}^2 < v^2 < v_{\mathbf{n}}^2. \tag{53}$$

The traction vector obtained in Eq. (25) can be written for the lower and upper half-spaces as,

$$\mathbf{t}^{\mathrm{LH}} = \mathbf{T}\mathbf{m} - A\rho v_{\mathbf{m}}^2 s_1\exp(-s_1\mathbf{m}\cdot\mathbf{x})\cos(k(\mathbf{n}\cdot\mathbf{x}-vt))\mathbf{a}, \tag{54}$$

and

$$\mathbf{t}^{\mathrm{UH}} = \mathbf{T}\mathbf{m} + D\rho v_{\mathbf{m}}^2 s_1\exp(s_1\mathbf{m}\cdot\mathbf{x})\cos(k(\mathbf{n}\cdot\mathbf{x}-vt))\mathbf{a}. \tag{55}$$

Similarly, the traction vector for the layer is given by

$$\tilde{\mathbf{t}} = \tilde{\mathbf{T}}\mathbf{m} + \tilde{\rho}\tilde{v}_{\mathbf{m}}^2 s_2(B\cos(s_2\mathbf{m}\cdot\mathbf{x}) - C\sin(s_2\mathbf{m}\cdot\mathbf{x}))\cos(k(\mathbf{n}\cdot\mathbf{x}-vt))\mathbf{a}. \tag{56}$$

In the time-dependent deformed state, at the interface $\mathbf{m}\cdot\mathbf{x} = \mathbf{m}\cdot\tilde{\mathbf{x}} = 0$, the continuity of the displacement and the traction are given by

$$\mathbf{u}^{\mathrm{LH}}(\mathbf{x},t) = \tilde{\mathbf{u}}(\mathbf{x},t) \quad \text{and} \quad \mathbf{t}^{\mathrm{LH}} = \tilde{\mathbf{t}}. \tag{57}$$

Similarly, at the interface $\mathbf{m}\cdot\mathbf{x} = \mathbf{m}\cdot\tilde{\mathbf{x}} = -h$, the continuity of the displacement and the traction vector are given by

$$\tilde{\mathbf{u}}(\mathbf{x},t) = \mathbf{u}^{\mathrm{UH}}(\mathbf{x},t) \quad \text{and} \quad \tilde{\mathbf{t}} = \mathbf{t}^{\mathrm{UH}}. \tag{58}$$

Substituting Eqs. (47), (49), (54), and (56) in Eq. (57) and using the continuity of traction given in Eq. (28b) yields

$$A - C = 0, \tag{59}$$

and

$$A\rho\, v_{\mathbf{m}}^2 s_1 + B\tilde{\rho}\,\tilde{v}_{\mathbf{m}}^2 s_2 = 0. \tag{60}$$

Next, substituting Eqs. (48), (49), (55), and (56) in Eq. (58) and using the continuity of traction given in Eq. (28b) yields

$$B\sin(s_2h) - C\cos(s_2h) + D\exp(-s_1h) = 0, \tag{61}$$

and

$$\tilde{\rho}\tilde{v}_{\mathbf{m}}^2 s_2 B\cos(s_2h) + \tilde{\rho}\tilde{v}_{\mathbf{m}}^2 s_2 C\sin(s_2h) - D\rho v_{\mathbf{m}}^2 s_1\exp(-s_1h) = 0. \tag{62}$$

The set of four homogeneous simultaneous equations with four unknowns A, B, C and D given in Eqs. (59)–(62) lead to the dispersion relation, which after some algebraic manipulation can be written as

$$\tan(s_2h) = \frac{2\rho v_{\mathbf{m}}^2\tilde{\rho}\tilde{v}_{\mathbf{m}}^2 s_1 s_2}{\tilde{\rho}^2\tilde{v}_{\mathbf{m}}^4 s_2^2 - \rho^2 v_{\mathbf{m}}^4 s_1^2}. \tag{63}$$

From Eqs. (42), (45), and (52), the relations

$$\frac{\rho v_{\mathbf{m}}}{\tilde{\rho}\tilde{v}_{\mathbf{m}}} = \frac{\rho_0 c}{\tilde{\rho}_0\tilde{c}}, \quad \frac{v_{\mathbf{n}}}{\tilde{v}_{\mathbf{n}}} = \frac{c}{\tilde{c}}, \tag{64}$$

can be obtained, where $c = \sqrt{\mu/\rho_0}$ and $\tilde{c} = \sqrt{\tilde{\mu}/\tilde{\rho}_0}$ are the transverse bulk wave speeds in the undeformed half-spaces and layer, respectively. Using Eq. (64) and the expressions for s_1 and s_2 defined in Eq. (50), the dispersion relation can be re-written as

$$\tan\left(kh(\tilde{v}_{\mathbf{n}}/\tilde{v}_{\mathbf{m}})\sqrt{\frac{v^2}{\tilde{v}_{\mathbf{n}}^2}-1}\right) = \frac{2\left(\frac{\rho_0 c}{\tilde{\rho}_0\tilde{c}}\right)\sqrt{\frac{c^2}{\tilde{c}^2}-\frac{v^2}{\tilde{v}_{\mathbf{n}}^2}}\sqrt{\frac{v^2}{\tilde{v}_{\mathbf{n}}^2}-1}}{\left(\frac{v^2}{\tilde{v}_{\mathbf{n}}^2}-1\right)-\left(\frac{\rho_0 c}{\tilde{\rho}_0\tilde{c}}\right)^2\left(\frac{c^2}{\tilde{c}^2}-\frac{v^2}{\tilde{v}_{\mathbf{n}}^2}\right)}. \tag{65}$$

When there is no pre-stress, $\mathbf{B} = \tilde{\mathbf{B}} = \mathbf{I}$, $J = \tilde{J} = 1$, hence $v_{\mathbf{m}} = v_{\mathbf{n}} = c$ in the half-spaces and $\tilde{v}_{\mathbf{m}} = \tilde{v}_{\mathbf{n}} = \tilde{c}$ in the layer, so that the dispersion relation given in Eq. (63) reduces to

$$\tan(kh\beta_2) = \frac{2\mu\tilde{\mu}\beta_1\beta_2}{\tilde{\mu}^2\beta_2^2 - \mu^2\beta_1^2}, \tag{66}$$

where $\beta_1 = \sqrt{1-v^2/c^2}$, $\beta_2 = \sqrt{v^2/\tilde{c}^2-1}$. Eq. (66) agrees with Eq. (8) of Stoneley (1924) and Eq. (4-232) of Ewing et al. (1957) when the upper and lower half-spaces are identical.

For a given left Cauchy–Green deformation tensor $\tilde{\mathbf{B}}$ in the layer and a given unit vector $\mathbf{m}$, there is, in general, only one propagation direction $\mathbf{n}$ in the interface along which a finite-amplitude shear horizontal wave may propagate. Indeed, because the two conditions $\mathbf{n}\cdot\mathbf{m} = 0$ and $\mathbf{n}\cdot\tilde{\mathbf{B}}\mathbf{m} = 0$ have to be satisfied, the propagation direction $\mathbf{n}$ must be along $\mathbf{m}\times\tilde{\mathbf{B}}\mathbf{m}$. In the case when $\mathbf{m}$ is along a principal axis of $\tilde{\mathbf{B}}$, then the two conditions $\mathbf{n}\cdot\mathbf{m} = 0$ and $\mathbf{n}\cdot\tilde{\mathbf{B}}\mathbf{m} = 0$ are automatically satisfied for any propagation direc-

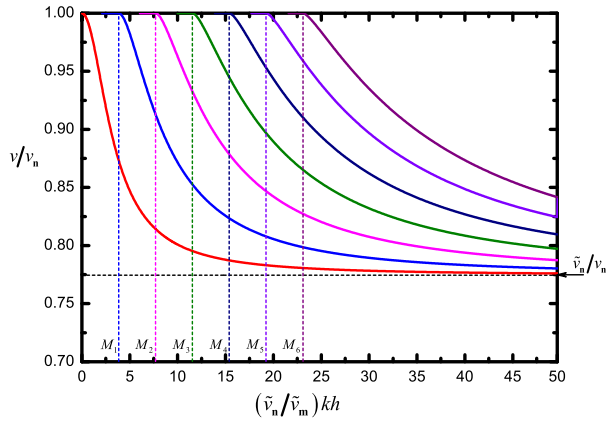

Fig. 2. Dispersion curves for finite-amplitude shear horizontal waves. Here, $M_n = n\pi/\sqrt{c^2/\tilde{c}^2 - 1}$, $(n = 1, 2, 3, \ldots)$. For $(\tilde{v}_\mathbf{m}/\tilde{v}_\mathbf{n})M_n < kh < (\tilde{v}_\mathbf{m}/\tilde{v}_\mathbf{n})M_{n+1}$, $n+1$ modes can propagate. Thus, for $0 < kh < (\tilde{v}_\mathbf{m}/\tilde{v}_\mathbf{n})M_1$, only one mode can propagate (fundamental mode).

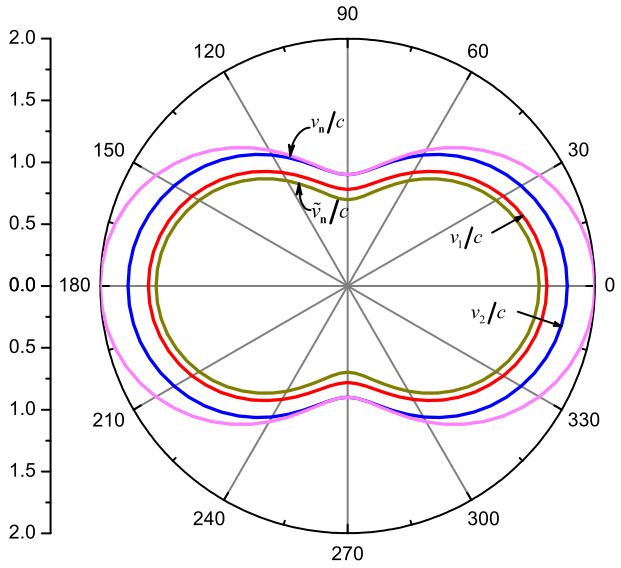

Fig. 3. Polar plots of the first two modes v_i/c, $(i = 1, 2)$ of the finite-amplitude shear horizontal wave speeds for Example 1 when $kh = \pi$. The homogeneous shear bulk wave speeds $v_\mathbf{n}/c$ and $\tilde{v}_\mathbf{n}/c$ are also shown.

tion $\mathbf{n}$ orthogonal to $\mathbf{m}$. Thus, the propagation direction $\mathbf{n}$ can be along any direction in the interface.

When the dispersion relation given in Eq. (63) is satisfied, the solution of the homogeneous equations given in Eqs. (59)–(62) for A, B, C and D can be written as

$$A = -\alpha\tilde{\rho}\tilde{v}_\mathbf{m}\kappa\exp(-\gamma h/v_\mathbf{m}), \tag{67a}$$

$$B = \alpha\rho v_\mathbf{m}\gamma\exp(-\gamma h/v_\mathbf{m}), \tag{67b}$$

$$C = -\alpha\tilde{\rho}\tilde{v}_\mathbf{m}\kappa\exp(-\gamma h/v_\mathbf{m}), \tag{67c}$$

$$D = -\alpha[\rho v_\mathbf{m}\gamma\sin(\kappa h/\tilde{v}_\mathbf{m}) + \tilde{\rho}\tilde{v}_\mathbf{m}\kappa\cos(\kappa h/\tilde{v}_\mathbf{m})], \tag{67d}$$

where α is an arbitrary constant which characterizes the amplitude of the shear horizontal wave. Let $(\eta,\ \xi,\ \zeta)$ denote the Cartesian coordinates along $(\mathbf{n},\ \mathbf{a},\ \mathbf{m})$ such that

$$\eta = \mathbf{n}\cdot\mathbf{x}, \quad \xi = \mathbf{a}\cdot\mathbf{x}, \quad \zeta = \mathbf{m}\cdot\mathbf{x}. \tag{68}$$

Using Eqs. (67) and (68), the displacement fields given in Eqs. (47)–(49) can be written in terms of α as

$$\mathbf{u}^{\mathrm{LH}}(\mathbf{x}, t) = -\alpha\tilde{\rho}\tilde{v}_\mathbf{m}\kappa\exp(-\gamma(h+\zeta)/v_\mathbf{m})\cos(k(\eta - vt))\mathbf{a}, \tag{69}$$

$$\mathbf{u}^{\mathrm{UH}}(\mathbf{x}, t) = -\alpha\exp(\gamma\zeta/v_\mathbf{m})[\rho v_\mathbf{m}\gamma\sin(\kappa h/\tilde{v}_\mathbf{m}) + \tilde{\rho}\tilde{v}_\mathbf{m}\kappa\cos(\kappa h/\tilde{v}_\mathbf{m})]\cos(k(\eta - vt))\mathbf{a}, \tag{70}$$

$$\tilde{\mathbf{u}}(\mathbf{x}, t) = \alpha\exp(-\gamma h/v_\mathbf{m})[\rho v_\mathbf{m}\gamma\sin(\kappa\zeta/\tilde{v}_\mathbf{m}) - \tilde{\rho}\tilde{v}_\mathbf{m}\kappa\cos(\kappa\zeta/\tilde{v}_\mathbf{m})]\cos(k(\eta - vt))\mathbf{a}, \tag{71}$$

or, equivalently, recalling Eq. (51),

$$\mathbf{u}^{\mathrm{LH}}(\mathbf{x}, t) = -\alpha\tilde{\rho}\tilde{v}_\mathbf{m}k\sqrt{v^2 - \tilde{v}_\mathbf{n}^2} \times \exp\left(-k(h+\zeta)\sqrt{\frac{v_\mathbf{n}^2 - v^2}{v_\mathbf{m}^2}}\right)\cos(k(\eta - vt))\mathbf{a}, \tag{72}$$

$$\mathbf{u}^{\mathrm{UH}}(\mathbf{x}, t) = -\alpha\exp\left(k\zeta\sqrt{\frac{v_\mathbf{n}^2 - v^2}{v_\mathbf{m}^2}}\right)\left[\rho v_\mathbf{m}k\sqrt{v_\mathbf{n}^2 - v^2}\sin\left(kh\sqrt{\frac{v^2 - \tilde{v}_\mathbf{n}^2}{\tilde{v}_\mathbf{m}^2}}\right) + \tilde{\rho}\tilde{v}_\mathbf{m}k\sqrt{v^2 - \tilde{v}_\mathbf{n}^2}\cos\left(kh\sqrt{\frac{v^2 - \tilde{v}_\mathbf{n}^2}{\tilde{v}_\mathbf{m}^2}}\right)\right]\cos(k(\eta - vt))\mathbf{a}, \tag{73}$$

$$\tilde{\mathbf{u}}(\mathbf{x}, t) = \alpha\exp\left(-kh\sqrt{\frac{v_\mathbf{n}^2 - v^2}{v_\mathbf{m}^2}}\right)\left(\rho v_\mathbf{m}k\sqrt{v_\mathbf{n}^2 - v^2}\sin\left(k\zeta\sqrt{\frac{v^2 - \tilde{v}_\mathbf{n}^2}{\tilde{v}_\mathbf{m}^2}}\right) - \tilde{\rho}\tilde{v}_\mathbf{m}k\sqrt{v^2 - \tilde{v}_\mathbf{n}^2}\cos\left(k\zeta\sqrt{\frac{v^2 - \tilde{v}_\mathbf{n}^2}{\tilde{v}_\mathbf{m}^2}}\right)\right)\cos(k(\eta - vt))\mathbf{a}. \tag{74}$$

Fig. 2 shows dispersion curves obtained from Eq. (65) for $\tilde{\rho}_0/\rho_0 = 1$ and $\tilde{\mu}/\mu = 0.6$. These dispersion curves are similar to linear isotropic elasticity, however, these curves have explicit dependence on the pre-stress. As stated in Eq. (53), the condition that the finite-amplitude shear horizontal waves can propagate within $\tilde{v}_\mathbf{n}$ and $v_\mathbf{n}$ can be observed clearly in Fig. 2 where the upper limit for the shear horizontal waves to propagate is the homogeneous bulk wave speed of the half-space $v_\mathbf{n}$. Since the wave speed

Table 1
Parameters for the layer and the half-spaces.

	Layer		Half-spaces	
	Principal stretches	Stress components	Principal stretches	Stress components
Example 1	$\tilde{\lambda}_1 = 2.0$, $\tilde{\lambda}_2 = 0.9$, $\tilde{\lambda}_3 = 0.7$	$\mathbf{e}_1\cdot\tilde{\mathbf{T}}\mathbf{e}_1 = 2.695\tilde{\mu}$, $\mathbf{e}_2\cdot\tilde{\mathbf{T}}\mathbf{e}_2 = 0.163\tilde{\mu}$, $\mathbf{e}_3\cdot\tilde{\mathbf{T}}\mathbf{e}_3 = -0.091\tilde{\mu}$,	$\lambda_1 = 2.0$, $\lambda_2 = 0.9$, $\lambda_3 = 0.709$	$\mathbf{e}_1\cdot\mathbf{T}\mathbf{e}_1 = 4.478\tilde{\mu}$, $\mathbf{e}_2\cdot\mathbf{T}\mathbf{e}_2 = 0.311\tilde{\mu}$, $\mathbf{e}_3\cdot\mathbf{T}\mathbf{e}_3 = -0.091\tilde{\mu}$,
Example 2	$\tilde{\lambda}_1 = 1.2$, $\tilde{\lambda}_2 = 0.8$, $\tilde{\lambda}_3 = 0.75$	$\mathbf{e}_1\cdot\tilde{\mathbf{T}}\mathbf{e}_1 = 0.44\tilde{\mu}$, $\mathbf{e}_2\cdot\tilde{\mathbf{T}}\mathbf{e}_2 = -0.671\tilde{\mu}$, $\mathbf{e}_3\cdot\tilde{\mathbf{T}}\mathbf{e}_3 = -0.779\tilde{\mu}$,	$\lambda_1 = 1.2$, $\lambda_2 = 0.8$, $\lambda_3 = 0.855$	$\mathbf{e}_1\cdot\mathbf{T}\mathbf{e}_1 = 0.6599\tilde{\mu}$, $\mathbf{e}_2\cdot\mathbf{T}\mathbf{e}_2 = -0.964\tilde{\mu}$, $\mathbf{e}_3\cdot\mathbf{T}\mathbf{e}_3 = -0.779\tilde{\mu}$,

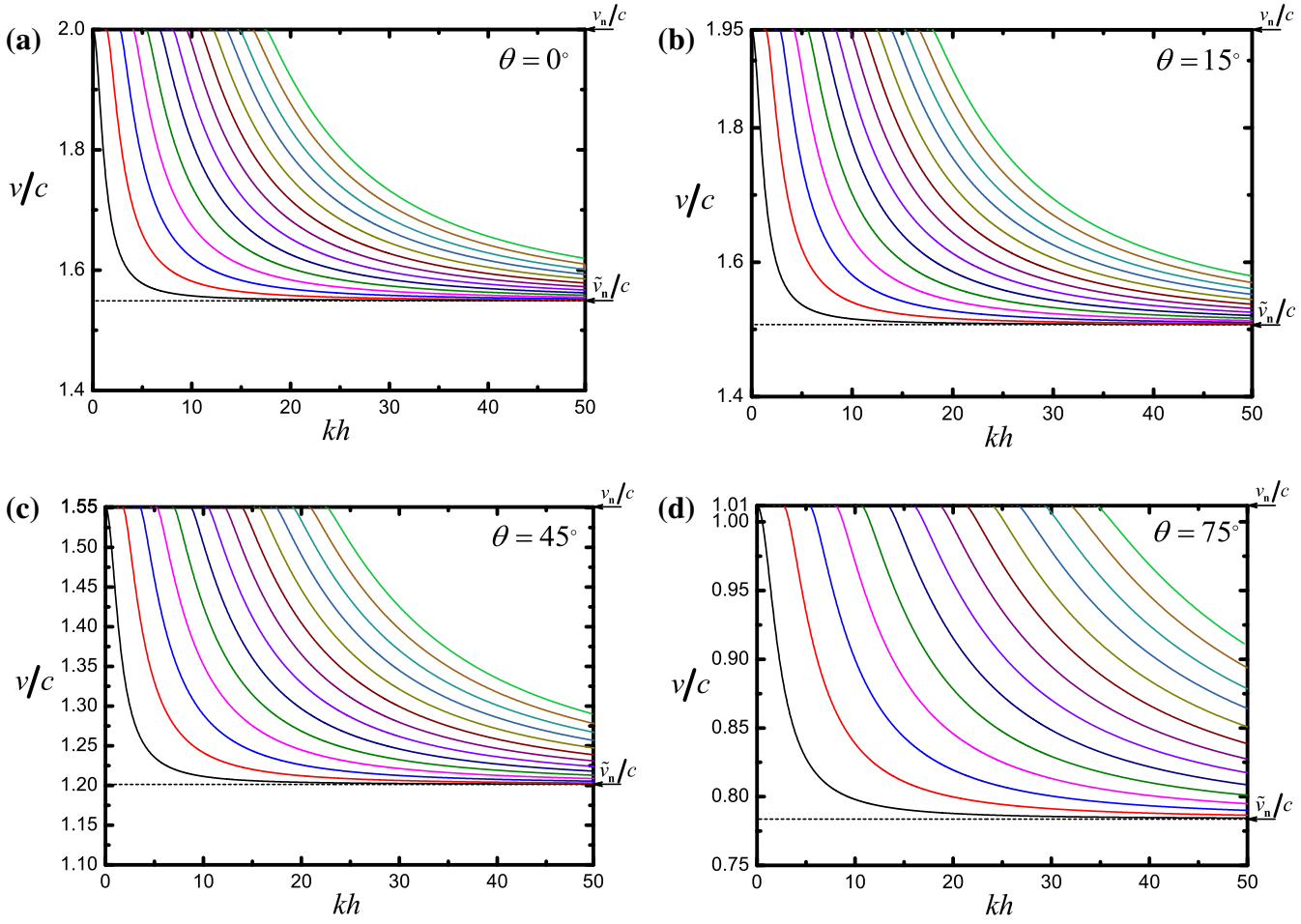

Fig. 4. Dispersion curves for the first 14 modes of Example 1 when (a) $\theta = 0^\circ$, (b) $\theta = 15^\circ$, (c) $\theta = 45^\circ$ and (d) $\theta = 75^\circ$.

is normalized with $v_{\mathbf{n}}$, the maximum value for each mode is 1 and the lower limit of the shear horizontal wave speed is $\tilde{v}_{\mathbf{n}}$. In contrast, for the dispersion curves due to *infinitesimal* wave propagation in a rigidly bonded layered pre-stressed composite, at the low wavenumber limit, at most two finite limiting phase speeds exist and the higher modes have infinite phase speeds. At the high wavenumber limit, the phase speed of the fundamental mode and the higher modes tend to Rayleigh surface wave speed, interfacial wave speed or the limiting phase speed of the composite (Kayestha et al., 2010).

5. Numerical results

As discussed in Section 4, when $\mathbf{m}$ is along a principal axis of $\tilde{\mathbf{B}}$, the propagation direction $\mathbf{n}$ can be along any direction in the interface. Numerical results obtained from the dispersion relation Eq. (65) are presented here for this special case.The unit vectors $\mathbf{e}_1$, $\mathbf{e}_2$ and $\mathbf{e}_3$ along the principal axes of $\tilde{\mathbf{B}}$ are given by

$$\mathbf{n} = \cos\theta\,\mathbf{e}_1 + \sin\theta\,\mathbf{e}_2, \quad \mathbf{a} = -\sin\theta\,\mathbf{e}_1 + \cos\theta\,\mathbf{e}_2, \quad \mathbf{m} = \mathbf{e}_3, \tag{75}$$

where θ is the angle which $\mathbf{n}$ makes with the direction $\mathbf{e}_1$, $\theta \in [0,\, 2\pi]$. In the pre-stressed layer, the left Cauchy–Green deformation tensor is given by

$$\tilde{\mathbf{B}} = \tilde{\lambda}_1^2\,\mathbf{e}_1 \otimes \mathbf{e}_1 + \tilde{\lambda}_2^2\,\mathbf{e}_2 \otimes \mathbf{e}_2 + \tilde{\lambda}_3^2\,\mathbf{e}_3 \otimes \mathbf{e}_3, \tag{76}$$

where $\tilde{\lambda}_1$, $\tilde{\lambda}_2$ and $\tilde{\lambda}_3$ are the principal stretches in the layer. Then, from Eqs. (42)–(46), the left Cauchy–Green deformation tensor $\mathbf{B}$ in the half-space can be written as

$$\mathbf{B} = \tilde{\lambda}_1^2\,\mathbf{e}_1 \otimes \mathbf{e}_1 + \tilde{\lambda}_2^2\,\mathbf{e}_2 \otimes \mathbf{e}_2 + \lambda_3^2\,\mathbf{e}_3 \otimes \mathbf{e}_3, \tag{77}$$

where $\lambda_3^2 = \tilde{\lambda}_1^{-2}\tilde{\lambda}_2^{-2}J^2$. Next, it is assumed that both the layer and the half-spaces are neo-Hookean materials of the Levinson and Burgess type where the material function is (Levinson and Burgess, 1971)

$$G^{\mathrm{LB}}(J) = (\lambda+\mu)(J^2-1) - 2(\lambda+2\mu)(J-1), \tag{78}$$

with $\mu > 0$ and $\lambda + \mu \geqslant 0$, which is consistent with Eq. (5). Using Eqs. (35) and (78) in Eq. (40), the expression for J can be obtained as

$$J = \frac{(\tilde{\lambda}+\tilde{\mu}+\tilde{\mu}\tilde{\lambda}_1^{-2}\tilde{\lambda}_2^{-2})\tilde{J} - (\tilde{\lambda}+2\tilde{\mu}) + (\lambda+2\mu)}{(\lambda+\mu+\mu\tilde{\lambda}_1^{-2}\tilde{\lambda}_2^{-2})}, \tag{79}$$

where $\tilde{J} = \tilde{\lambda}_1\tilde{\lambda}_2\tilde{\lambda}_3$ and λ, μ and $\tilde{\lambda}$, $\tilde{\mu}$ are the Lamé parameters of the half-spaces and the layer, respectively. The corresponding Cauchy stress tensor for the layer and the half-spaces are given by

$$\begin{aligned}\tilde{\mathbf{T}} = {} & (\tilde{\mu}\tilde{J}^{-1}\tilde{\lambda}_1^2 + \tilde{J}(\tilde{\lambda}+\tilde{\mu}) - (\tilde{\lambda}+2\tilde{\mu}))\mathbf{e}_1 \otimes \mathbf{e}_1 \\ & + \left(\tilde{\mu}\tilde{J}^{-1}\tilde{\lambda}_2^2 + \tilde{J}(\tilde{\lambda}+\tilde{\mu}) - (\tilde{\lambda}+2\tilde{\mu})\right)\mathbf{e}_2 \otimes \mathbf{e}_2 + (\tilde{\mu}\tilde{J}^{-1}\tilde{\lambda}_3^2 + \tilde{J}(\tilde{\lambda} \\ & + \tilde{\mu}) - (\tilde{\lambda}+2\tilde{\mu}))\mathbf{e}_3 \otimes \mathbf{e}_3,\end{aligned} \tag{80}$$

and

$$\begin{aligned}\mathbf{T} = {} & (\mu J^{-1}\tilde{\lambda}_1^2 + J(\lambda+\mu) - (\lambda+2\mu))\mathbf{e}_1 \otimes \mathbf{e}_1 \\ & + \left(\mu J^{-1}\tilde{\lambda}_2^2 + J(\lambda+\mu) - (\lambda+2\mu)\right)\mathbf{e}_2 \otimes \mathbf{e}_2 + (\mu J^{-1}\lambda_3^2 + J(\lambda \\ & + \mu) - (\lambda+2\mu))\mathbf{e}_3 \otimes \mathbf{e}_3,\end{aligned} \tag{81}$$

respectively. In addition, using Eqs. (52), (75), (76), and (77), the homogeneous bulk wave speeds for the layer and the half-spaces can be written as

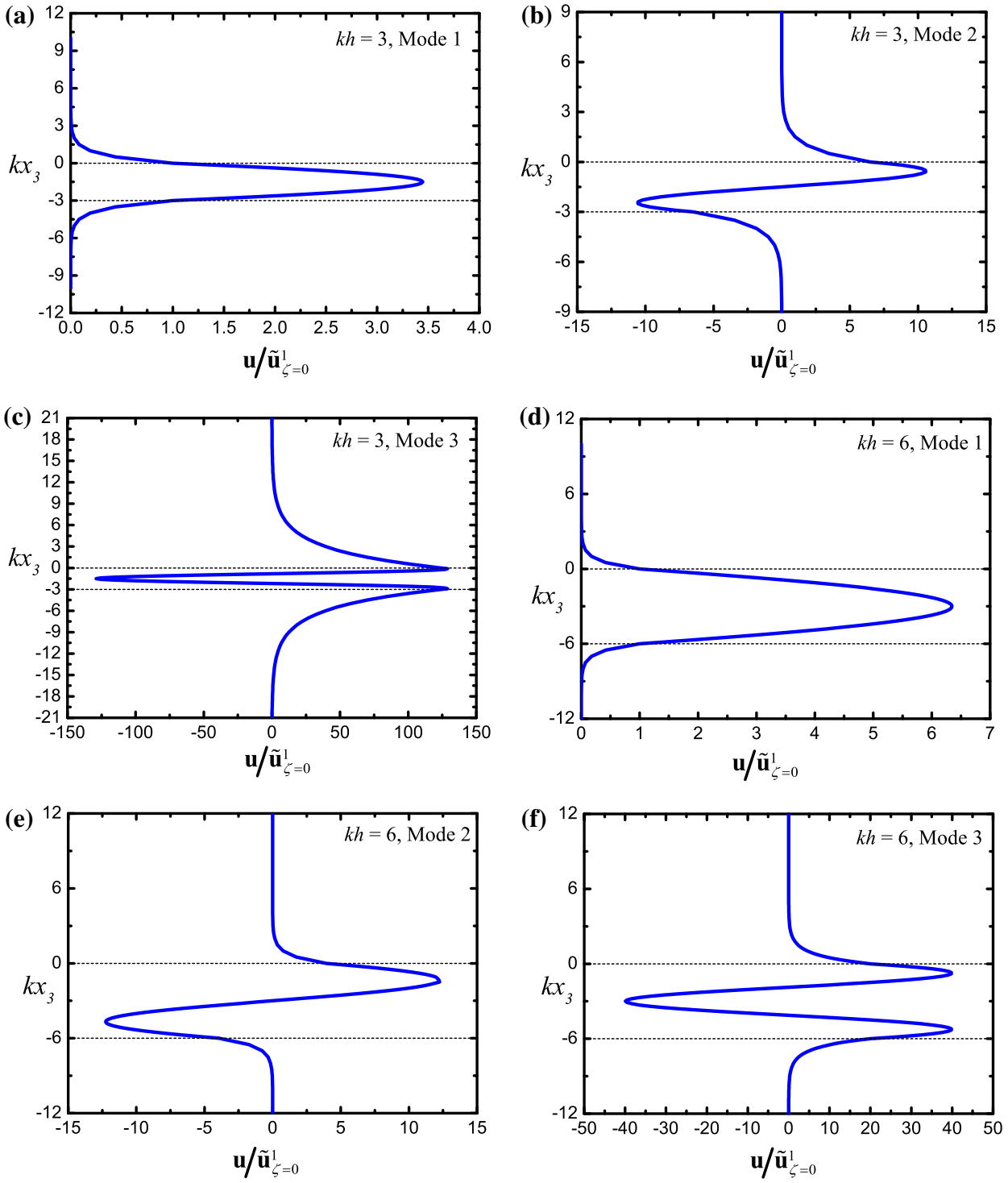

Fig. 5. Displacements normalized by $\tilde{\mathbf{u}}^1_{\zeta=0}$ for $kh = 3$ and $kh = 6$ when $\theta = 0^\circ$ for Example 1.

$$\tilde{v}_{\mathbf{n}}^2/\tilde{c}^2 = v_{\mathbf{n}}^2/c^2 = \tilde{\lambda}_1^2\cos^2\theta + \tilde{\lambda}_2^2\sin^2\theta,$$
$$\tilde{v}_{\mathbf{m}}^2/\tilde{\lambda}_3^2\tilde{c}^2 = v_{\mathbf{m}}^2/\lambda_3^2 c^2 = 1. \tag{82}$$

Two numerical examples have been considered in which Example 1 corresponds to the case of a volume increase while Example 2 corresponds the case of a volume decrease. The layer and the half-spaces are chosen such that $\tilde{\rho}_0/\rho_0 = 1$ and $\tilde{\mu}/\mu = 0.6$. Polar plots are given for the finite-amplitude shear horizontal waves $kh = \pi$, which refers to wavelength twice the thickness of the layer. The wave speeds are normalized with the transverse bulk wave speed in the undeformed half-space, c. In addition, dispersion curves for the propagation angles $\theta = 0^\circ$, 15°, 45° and 75° are given for the first 14 modes. The prescribed parameters $\tilde{\lambda}_1, \tilde{\lambda}_2, \tilde{\lambda}_3$ and the computed parameters $\mathbf{e}_1 \cdot \tilde{\mathbf{T}}\mathbf{e}_1$, $\mathbf{e}_2 \cdot \tilde{\mathbf{T}}\mathbf{e}_2$, $\mathbf{e}_3 \cdot \tilde{\mathbf{T}}\mathbf{e}_3$, $\lambda_1 = \tilde{\lambda}_1$, $\lambda_2 = \tilde{\lambda}_2$, $\lambda_3 = \tilde{\lambda}_1^{-1}\tilde{\lambda}_2^{-1}J$, $\mathbf{e}_1 \cdot \mathbf{T}\mathbf{e}_1, \mathbf{e}_2 \cdot \mathbf{T}\mathbf{e}_2, \mathbf{e}_3 \cdot \mathbf{T}\mathbf{e}_3$ are shown in Table 1. The Lamé parameters for the layer and the half-spaces are chosen such that $\tilde{\lambda} = \tilde{\mu}$ and $\lambda = \mu$.

5.1. Example 1

The layer undergoes a volume increase of 26% and the half-spaces undergo a volume increase of 27.6%. Fig. 3 shows the

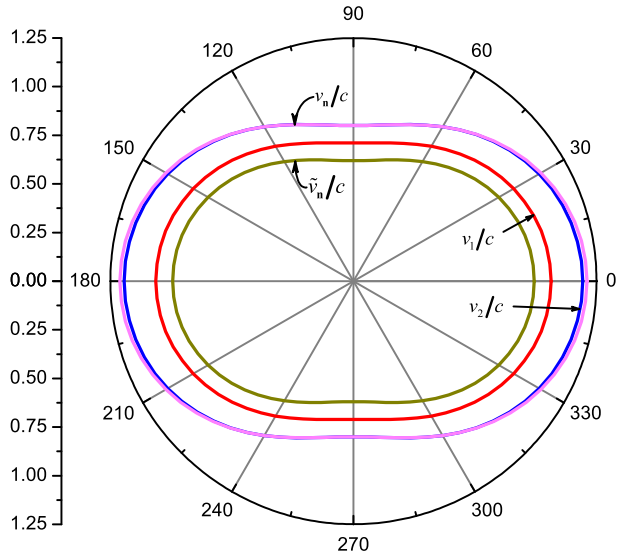

Fig. 6. Polar plots of the first two modes v_i/c, $(i = 1, 2)$ of the finite-amplitude shear horizontal wave for Example 2 when $kh = \pi$. The homogeneous shear bulk wave speeds $v_{\mathbf{n}}/c$ and $\tilde{v}_{\mathbf{n}}/c$ are also shown.

variation of finite-amplitude shear horizontal wave speeds with the propagation angle θ. It can be seen that the first two modes of the finite-amplitude shear horizontal waves can propagate for any angle θ, within $\tilde{v}_{\mathbf{n}}/c$ to $v_{\mathbf{n}}/c$. In addition, it can be observed that the wave speeds of the finite-amplitude shear horizontal waves depend on the pre-stretch with maximum wave speed corresponding to the maximum stretch and minimum wave speed corresponding to the minimum stretch. Fig. 4 shows the dispersion curves where it can be seen that, with increasing kh the number of modes that can propagate within $\tilde{v}_{\mathbf{n}}/c$ to $v_{\mathbf{n}}/c$ increases and the number of modes differ with the propagation angle.

The first three modes of displacement fields given in Eqs. (72)–(74) are plotted in Fig. 5 for $kh = 3$ and $kh = 6$ when $\theta = 0°$. Note that the maximum number of modes that can propagate at $\theta = 0°$ are 3 modes for $kh = 3$ and 6 modes for $kh = 6$ (see Fig. 4(a)). The displacements which have been normalized by the first mode displacement of the layer at $\zeta = 0$, clearly show that the higher modes penetrate further into the lower and upper half-spaces.

5.2. Example 2

In this example, the layer undergoes a volume decrease of 28% and the half-spaces undergo a volume decrease of 18%. The polar plots showing the variation of shear horizontal wave speeds with the propagation direction $\mathbf{n}$ for $kh = \pi$ are presented in Fig. 6. It can be observed that only the first two modes of the finite- amplitude shear horizontal waves can propagate for all propagation directions within $\tilde{v}_{\mathbf{n}}/c$ to $v_{\mathbf{n}}/c$. Comparing Figs. 4 and 7, it can be seen that for the same propagation angle, the homogeneous bulk wave speeds of the layer and the half-space are larger in Example

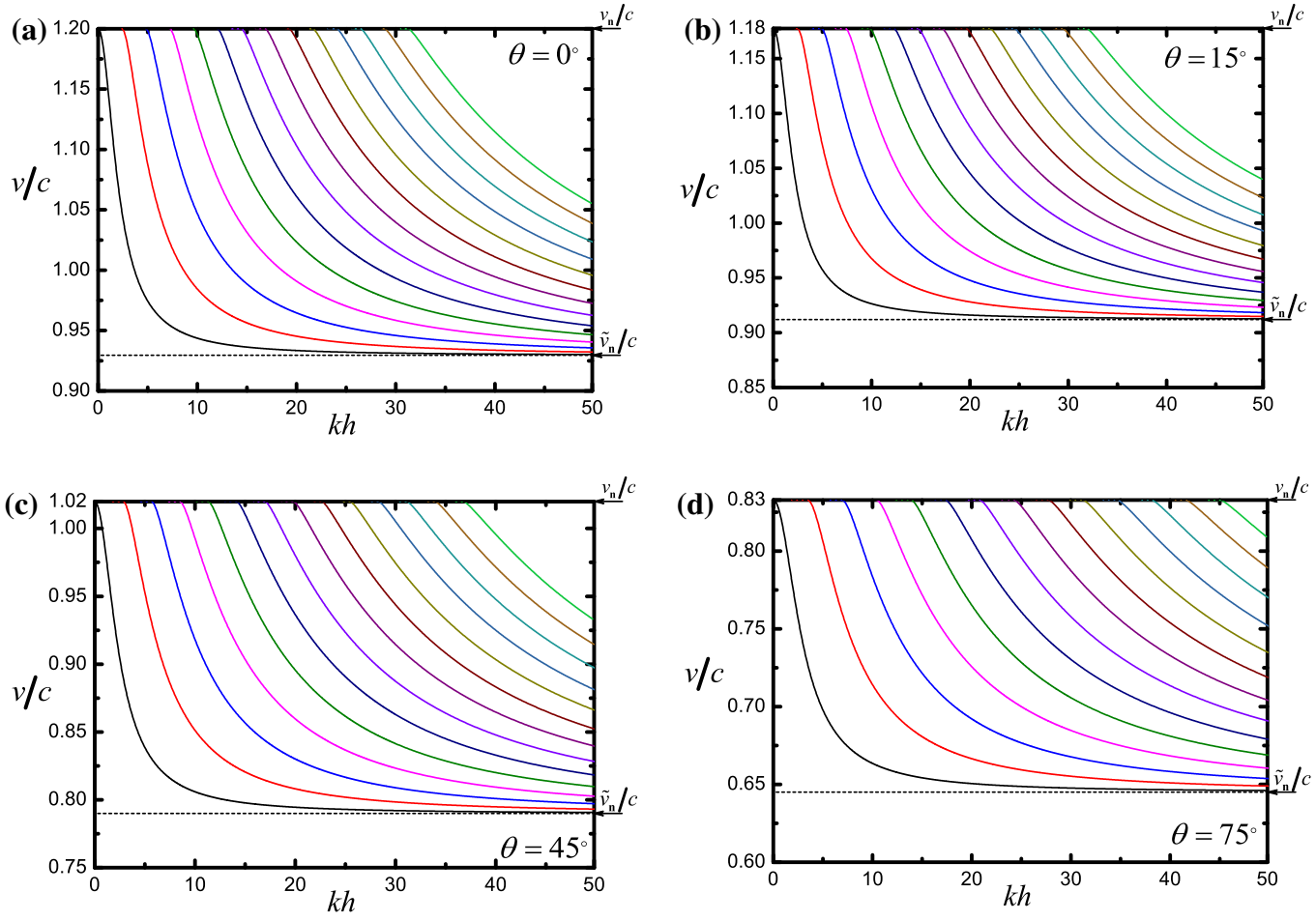

Fig. 7. Dispersion curves for the first 14 modes of Example 2 when (a) $\theta = 0°$, (b) $\theta = 15°$, (c) $\theta = 45°$ and (d) $\theta = 75°$.

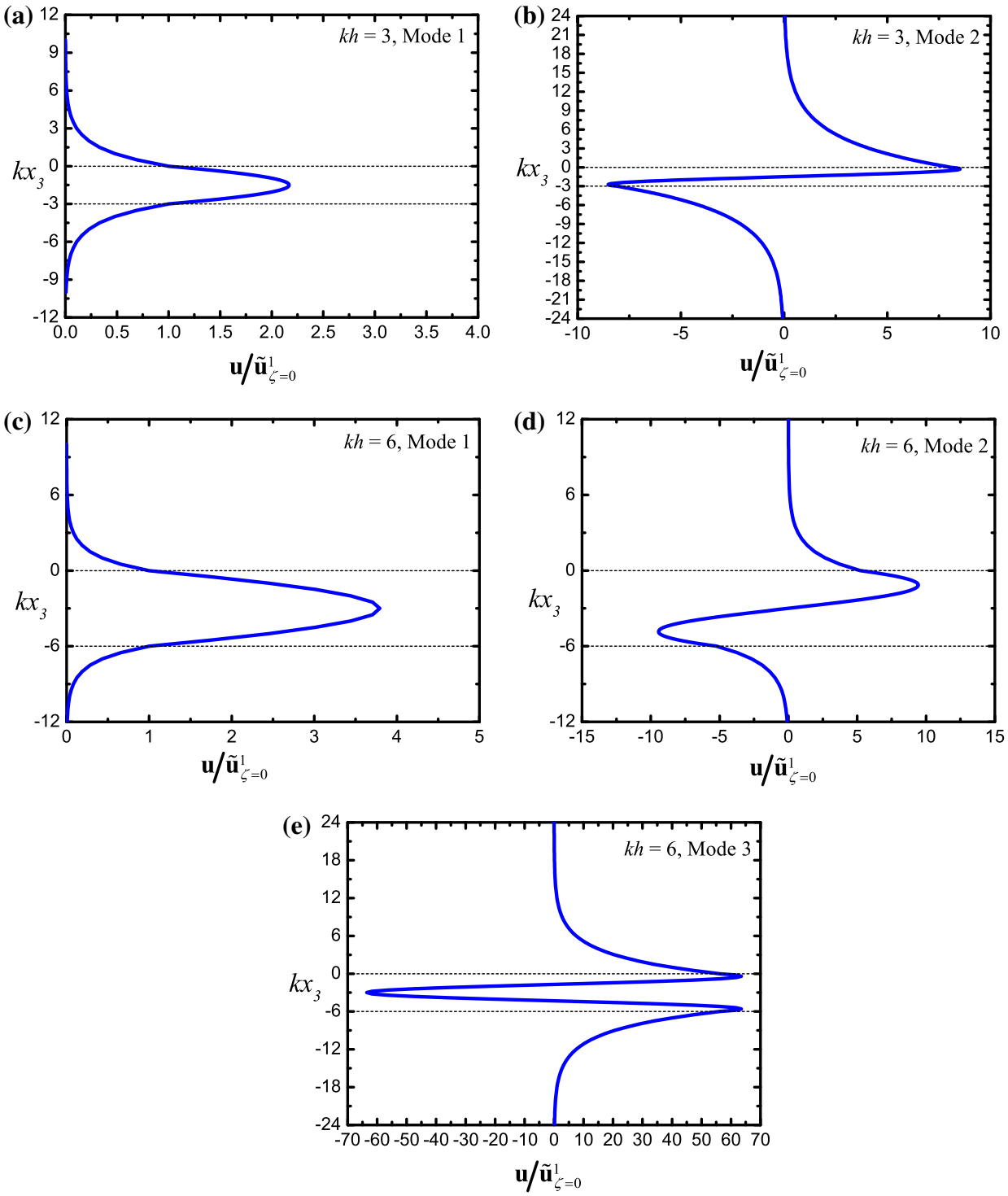

Fig. 8. Displacements normalized by $\tilde{\mathbf{u}}^1_{\zeta=0}$ for $kh = 3$ and $kh = 6$ when $\theta = 0^\circ$ for Example 2.

1 than in Example 2, which is due to the pre-stretch. The influence of the pre-stretch can be seen in these figures which imply that the pre-stress leading to volume increase results in an increase of the wave speed. Larger the homogenous bulk wave speeds, larger are the wave speeds of the shear horizontal wave, as these wave speeds are within the range of the homogeneous bulk wave speeds of the layer and the half-space.

The displacement fields given by Eqs. (72)–(74) are plotted in Fig. 8 for $kh = 3$ and $kh = 6$ when $\theta = 0^\circ$. The maximum number of modes that can propagate are 2 modes for $kh = 3$ and 3 modes for $kh = 6$ (see Fig. 7(a)). Here too, it can be seen from the displacement profiles, which have been normalized by the amplitude of the first mode, that the higher modes penetrate further into the half-spaces.

6. Summary and conclusions

In this paper, the dispersion relation for finite-amplitude shear horizontal waves propagating in a pre-stressed layer embedded between two identical half-spaces made of pre-stressed compressible

neo-Hookean materials has been obtained in explicit form. It has been shown that, finite-amplitude shear horizontal waves may propagate, provided that the direction of normal to the planes of constant phase and the direction of normal to the planes of constant amplitude are conjugate with respect to the **B**-ellipsoid and $\tilde{\mathbf{B}}$-ellipsoid, where **B** and $\tilde{\mathbf{B}}$ are the left Cauchy–Green deformation tensors corresponding to the initial deformation of the half-spaces and the layer, respectively. Numerical results are presented for the special case when the interfaces are principal planes of left Cauchy–Green deformation tensor. It has been observed that the wave speeds of the shear horizontal waves are larger when the layer and the half-space undergo volume increase, which is true for all the propagation directions. In addition, it has also been observed that the number of modes propagating for a particular *kh* value differ with the propagation angle.

Acknowledgements

PK and ACW acknowledge financial support from the Center for Urban Earthquake Engineering (CUEE) through the GCOE program "International Urban Earthquake Engineering Center for Mitigating Seismic Mega Risk". The authors are grateful to Professor Philippe Boulanger for useful discussions regarding this paper. ERF also acknowledges Professor Graham A. Rogerson for the encouragement and suggestion to work on the subject of this paper.

References

Beatty, M.F., 1996. Introduction to nonlinear elasticity. In: Carroll, M.M., Hayes, M.A. (Eds.), Nonlinear Effects in Fluids and Solids. Plenum Press, New York, pp. 13–112.

Boulanger, Ph., Hayes, M., Trimarco, C., 1994. Finite-amplitude plane waves in deformed Hadamard elastic materials. Geophys. J. Int. 118, 447–458.

Chadwick, P., 1999. Continuum Mechanics. Dover, New York.

Currie, P., Hayes, M., 1969. Longitudinal and transverse waves in finite elastic strain. Hadamard and Green materials. J. Inst. Math. Appl. 5, 140–161.

Destrade, M., 1999. Finite-amplitude inhomogeneous plane waves in a deformed Blatz-Ko material, in: Croitoro, E.M. (Ed.), Proceedings of the First Canadian Conference on Nonlinear Solid Mechanics, University of Victoria Press, Victoria, vol. 1, pp. 89–98.

Destrade, M., Saccomandi, G., 2005. Finite amplitude elastic waves propagating in compressible solids. Phys. Rev. E72, 016620.

Destrade, M., Saccomandi, G., 2010. Waves in Nonlinear Pre-stressed Materials. CISM Courses and Lectures, vol. 495, Springer, Udine.

Ewing, W.M., Jardetzky, W.S., Press, F., 1957. Elastic Waves in Layered Media. McGraw-Hill, New York.

Hayes, M., 1968. A remark on Hadamard materials. Quart. J. Mech. Appl. Math. 21, 141–146.

John, F., 1966. Plane elastic waves of finite amplitude. Hadamard materials and harmonic materials. Commun. Pure Appl. Math. 19, 309–341.

Kayestha, P., Wijeyewickrema, A.C., Kishimoto, K., 2010. Time-harmonic wave propagation in a pre-stressed compressible elastic bi-material laminate. Eur. J. Mech. A: Solids 29, 143–151.

Levinson, M., Burgess, I.W., 1971. A comparison of some simple constitutive relations for slightly compressible rubber-like materials. Int. J. Mech. Sci. 13, 563–572.

Rodrigues Ferreira, E., Boulanger, Ph., 2005. Finite-amplitude damped inhomogeneous waves in a deformed Blatz-Ko material. Math. Mech. Solids 10, 377–387.

Rodrigues Ferreira, E., Boulanger, Ph., 2007. Superposition of transverse and longitudinal finite-amplitude waves in a deformed Blatz-Ko material. Math. Mech. Solids 12, 543–558.

Rodrigues Ferreira, E., Boulanger, Ph., Destrade, M., 2008. Large-amplitude Love waves. Quart. J. Mech. Appl. Math. 61, 353–371.

Stoneley, R., 1924. Elastic waves at the surface of separation of two solids. Proc. R. Soc. A 106, 416–428.

Willson, A.J., 1977. Plate waves in Hadamard materials. J. Elast. 7, 103–111.

Wijeyewickrema, A.C., Leungvichcharoen, S., 2009. Wave propagation in pre-stressed imperfectly bonded compressible elastic layered composites. Mech. Mat. 41, 1192–1203.